Journal of Machine Construction and Maintenance
PROBLEMY EKSPLOATACJI
QUARTERLY ISSN 1232-9312 1/2017 (104)
p. 29–35

Tomasz TOMASZEWSKI, Janusz SEMPRUCH
UTP University of Science and Technology, Bydgoszcz, Poland
tomaszewski@utp.edu.pl, janusz.sempruch@utp.edu.pl

SIZE EFFECT IN HIGH-CYCLE FATIGUE

Key words: high-cycle fatigue, size effect minispecimen, aluminium alloy.

Abstract: The paper describes size effect in reference to available empirical and analytical models. The size effect of an object on strength properties was classified from 3 perspectives: statistical, geometrical, and technological. The following part of the paper identifies a verification method that has been supplemented by proprietary experimental test results obtained for a minispecimen made of aluminium alloy EN AW-6063.

Efekt skali w zmęczeniu wysokocyklowym

Słowa kluczowe: zmęczenie wysokocyklowe, efekt skali, minipróbka, stop aluminium.

Streszczenie: Artykuł przedstawia efekt skali w odniesieniu do dostępnych modeli empirycznych i analitycznych. Wpływ efektu skali na wytrzymałość zmęczeniową obiektu został sklasyfikowany z trzech różnych perspektyw: statystycznej, geometrycznej oraz technologicznej. W artykule zidentyfikowano metodę weryfikacji, która została uzupełniona przez wyniki badań eksperymentalnych dla minipróbki stopu aluminium EN AW-6063.

Introduction

Fatigue properties are identified for miniature specimens (Fig. 1, area a I), standard specimens (Fig. 1, area a II), and for real large objects (Fig. 1, area a III).

These objects will have different strengths as a result of the size effect, among other factors. Based on many experimental studies, it was confirmed that strength is inversely proportional to the size of an object subjected to monotonic or fatigue loads (Fig. 1b: n – standard specimen, m – minispecimen, r – real large object) [1]. The decrease or increase in strength is explained by the effect of factors related to the random distribution of flaws in the material, shape, load type, and object production processes. The size effect is so important that it has to be considered in the engineering practice.

Fatigue properties are typically identified based on the testing of standard specimens, which is shown schematically in Fig. 1c in the form of a quantitative distribution of the probability of obtaining experimental data depending on cross-sections of tested specimens or real-life objects.

The sensitivity of a material to size effect is described using the cross-section area coefficient K, where the presentation of which depends on the nature or type of tests [2] as follows:

$$K_Z = \frac{\sigma_{(-1)}}{\sigma_{(-1)n}},\ K_{HC} = \frac{\sigma}{\sigma_n},\ K_S = \frac{S_u}{S_{un}} \qquad (1a, b, c)$$

where

$Z/\sigma/S_u$ – fatigue limit/fatigue strength/ultimate tensile strength of a specimen with any cross-section,

$Z_n/\sigma_n/S_{un}$ – fatigue limit/fatigue strength/ultimate tensile strength of a normative specimen (cross-section 20–80 mm^2) prepared using an identical material.

The cited definitions refer to a specific plane for which stress is determined. The working part of the specimen is the place for averaging values for the specific volume.

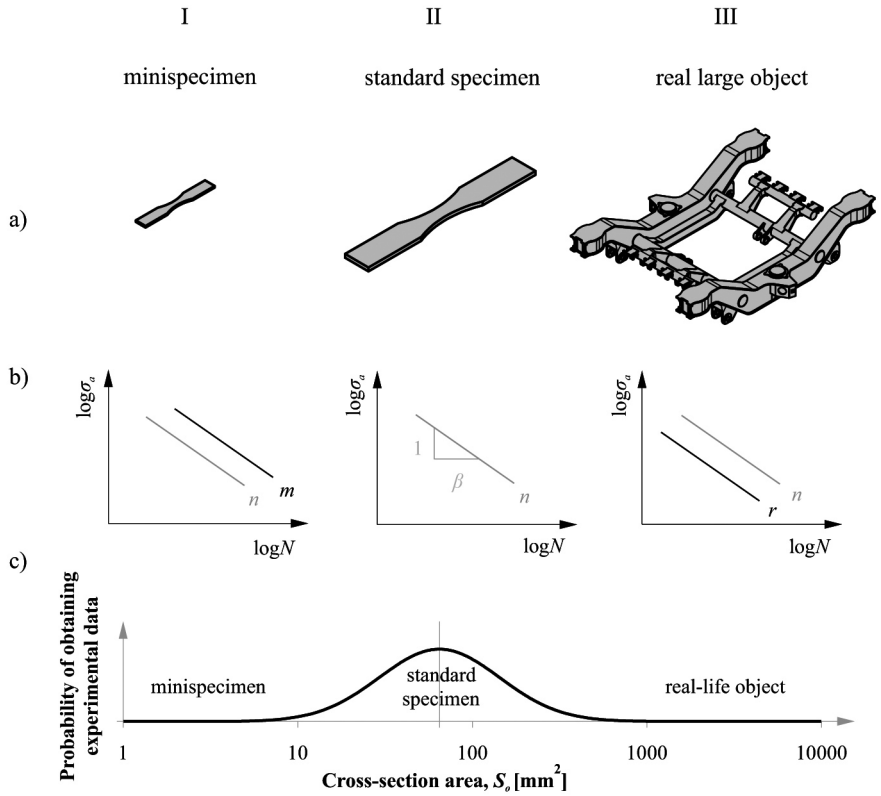

Fig. 1. Size effect – visualization of the problem

1. Size effect in empirical approach

Figure 2 shows, in a graphic form, the change of the K_z coefficient for the specimen diameter notwithstanding the load type. See Table 1 for a more extensive list of values of K_z. The cited dependencies are applied to a range of object sizes and allow the determination of the cross-section area coefficient K_z for the fatigue limit.

The source of the size effect is often explained based on the influence of the stress gradient (deformation) occurring under bending and shear stress. Because the stress gradient does not occur in axially loaded specimens, some studies (e.g., [4] and [5]) assumed that there was no need for using the coefficient of the size effect. However, direct fatigue tests have demonstrated that the size effect does have a slight influence on axially loaded components and using it is recommended [6, 7, 8].

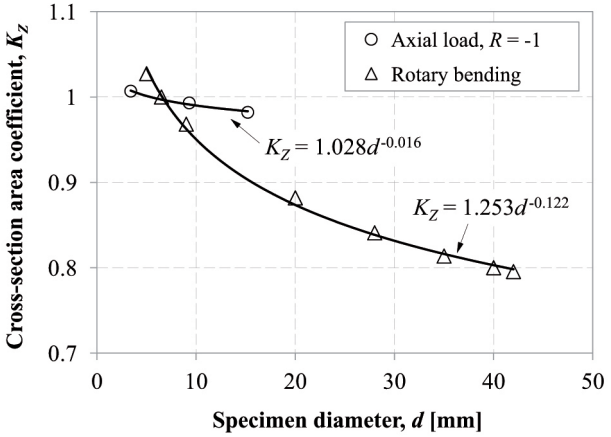

Fig. 2. The influence of size effect on axial load and rotary bending of specimens made of low-alloy steel – proprietary study based on [3]

Table 1. Quantitative dependencies of the cross-section area coefficient K_Z [4]

K_Z	Range [mm]	Author
$\frac{0.947}{1-0.406/d}$	$3.2 \le d \le 48$	Moore
$0.931\left(1+\frac{0.014}{0.1+(d/25.4)^2}\right)$	$d \le 50$	Heywood
1 $1.189\,d^{-0.097}$ 0.6	$d \le 8$ $8 \le d \le 250$ $d \ge 250$	Shigley & Mitschke
1 0.9 0.8 0.7	$d \le 10$ $10 < d < 50$ $50 < d < 100$ $100 < d < 150$	Juvinall
$1-\frac{d-7.62}{381}$	$50 \le d \le 230$	Roark

2. Classification of analytical models

2.1. Statistical

The statistical theory of the weakest link uses Weibull's distribution of the probability of destruction. The model has been presented in study [9] and analysed in study [2]. This weakest link theory used a function of the distribution of a two-dimensional distribution of the probability of "damaging the function" dependent on the number of cycles ($P(\log N)$). The distribution of fatigue strength for a given stress level is described in a logarithmic scale [3] and expressed with the following relation (designations of characteristic quantities conforming to the original studies have been retained in the following models):

$$P(N) = 1 - \exp\left[-\left(\frac{\log(N)}{\log(N_0)}\right)^m\right] \tag{2}$$

where

N_0 – reference fatigue strength (for probability 0.63) for a given stress level,

m – distribution form coefficient responsible for the width of the band of scatter of fatigue strength N.

The model assumes that results for specimens with different cross-sectional areas are linked one to another. It is assumed that the distribution from coefficient m, and the scale coefficient N_0, are material constants independent of the specimen size and stress distribution. The following relation can be applied to the same quantities (probability of destruction and stress distribution) and two different specimen sizes:

$$\frac{N_2}{N_1} = \left(\frac{S_{o1}}{S_{o2}}\right)^{\frac{1}{m}} \tag{3}$$

where

N_1 – fatigue strength for a specimen with a known cross-section area S_{o1},

N_2 – estimated fatigue strength for a specimen with the sought cross-section area S_{o2}.

The monofractal approach is another statistical model of the size effect, which assumes modelling of damage to the material structure. The model has been presented in study [1] and analysed in study [2]. From the macroscopic point of view, a fatigue fracture is similar to a simple incision of length a. It is modelled after the determinist "invasive" set of fractals featuring a geometry referring to the von Koch's curve (Fig. 3).

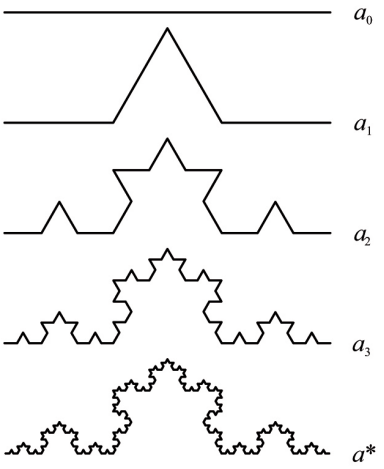

Fig. 3. Reference fracture shape depending on the scale of observation for sets of fractals [1]

The application of the monofractal approach to high-cycle fatigue is based on the Basquin's equation. The following relation was proposed for the assumed parallelism of the σ_a-N characteristics determined for different specimen sizes specimens [1]:

$$C_B = C_A \left(\frac{D_A}{D_B} \right)^{-d_f \beta} \tag{4}$$

where
D_A, D_B – characteristic dimensions for geometrically similar specimens A and B assuming that $D_B > D_A$,
C_A, C_B – constant parameters of characteristic σ_a-N,
$d_f\beta$ – straight line slope (Fig. 4).

The relation of the characteristic dimension to the material structure was described by equation $\alpha = 2 - d_f$ for $0 < d_f < 0.5$. Assuming that $D_A = 1$, $D_B = D$, and determinations of $C_A = C_1$ for accepted dimension $D = 1$, expression (4) can be written in the following generic form [1]:

$$C(D) = C_1 (D)^{-d_f \beta} \tag{5}$$

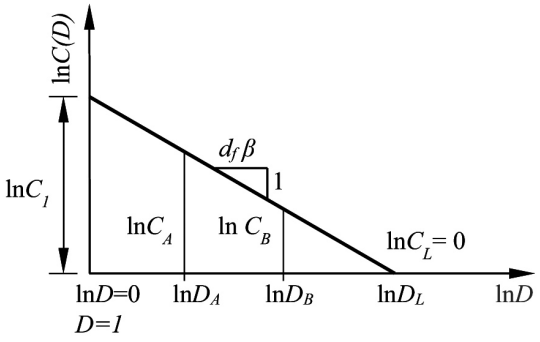

Fig. 4. The dependency of the parameter $C(D)$ of characteristic σ_a-N on dimension D in bilogarithmic scale

Equations (4) and (5) describe the linear sensitivity of a material or group of materials to change in the cross-section area. The location of characteristics $C(D)$-D with slope $d_f\beta$ is determined based on constant parameters C of individual characteristics σ_a-N for specimens that are different in size. The monofractal approach has no upper and lower limits with respect to scaling. It is true only within a narrow range of object sizes (dimensions).

2.2.Geometrical

The geometrical expression of the size effect is related to the non-linear distribution of stress with the high peak stress value or load type. For various specimen sizes, fatigue properties of the material are described using the volumetric method. The model is based on highly stressed volume $V_{n\%}$ that features a higher probability of the initiation of the fracture or aggravation of the existing flaw. The model is presented in the form of a linear dependency of the logarithm of local stress amplitude and the logarithm of highly stressed volume [10]:

$$\sigma_a = A V_{n\%}^{-v} \tag{6}$$

where
A, v – material-independent parameters,
$V_{n\%}$ – highly stressed volume for n = 95, 90.

For any relation of $V_{n\%}$, equation (6) can be written in the following form:

$$\frac{\sigma_{a,1}}{\sigma_{a,2}} = \left(\frac{V_{n\%,1}}{V_{n\%,2}} \right)^{v} \tag{7}$$

where
$\sigma_{a,1}$, $\sigma_{a,2}$ – fatigue strength of a specimen volume $V_{n\%,1}$, $V_{n\%,2}$.

Equations (6) and (7) are valid for a specific σ_0 limit below which there is no fatigue strength drop. The value of σ_0 corresponds to the lower boundary volume V_0, where the accepted value ranges from 30 to 60 mm^3 [11].

2.3. Technological

Fatigue properties are strongly correlated to the distribution of flaws in a material. Non-metallic inclusions degrade the strength of even very pure high-resistance steel grades. From the point of view of the study of the size effect, it is necessary to determine the distribution of flaw sizes depending on object size. The number of flaws in test specimens is so large that it is possible to determine the statistical distribution of the flaws for extreme values.

The method consists in determining the characteristic size of the largest flaw existing within the examined area. The probability of the non-occurrence of flaw size x in n tests results from the calculus of probability and is described by the Gumbel's distribution [12]:

$$P(x) = \exp\left[-\exp\left(-\frac{(x - \lambda)}{\delta} \right) \right]^{n} \tag{8}$$

where
λ – parameter of the location of the distribution,
δ – parameter of the scale,
n – number of observations, ratio of the surface of the larger specimen to that of the smaller one, $n = S_o/S_{on}$.

Assuming a quintile of the order of P for the largest flaw X_P in the control specimen of surface S_{on}, we obtain the following relation [12]:

$$X_{P0} = \lambda - \delta\left[\ln\left(-\ln\left(P^{1/n}\right)\right)\right] \tag{9}$$

and, for the tested specimen with surface S_o:

$$X_P = \lambda - \delta\left[\ln\left(-\ln P\right)\right] \tag{10}$$

The size of the specimen is described by an adjustment coefficient depending on n [12] as follows:

$$K = \frac{X_P}{X_{P0}} \tag{11}$$

Quantities λ and δ are parameters of the distribution of the function of flaws for the control specimen. The cited relations enable analysing the size effect for specimens larger than the control ones. A change in the direction of analyses (for smaller specimens) is done by reversing the X_{P0}/X_P ratio.

3. Verification components

3.1. Verification method

The verification was done assuming the existence of the following:

a) An actual situation in a structural component: Fig. 5;
b) Experimental data for the minispecimen: Fig. 1, area I a;
c) Experimental data for the standard specimen: Fig. 1, area II a;
d) A verified and approved analytical model based on which analytical data for the standard specimen shown in Fig. 1, area II a, were determined using data provided in Fig. 1, area I a.

The monofractal model presented in subsection 3.1 was accepted as the verified method referred to in paragraph (d). This selection was made based on experience learned within study [13].

3.2. Experimental data for verification

Tests were performed on non-standard specimens geometrically smaller than the reference one (minispecimen). The purpose of developing such tests ensues from the need of performing the tests for hitherto inaccessible areas. This applies to the impossibility of collecting specimens due to limited object sizes. See the thin-walled shaped sections shown in Fig. 5 for an example.

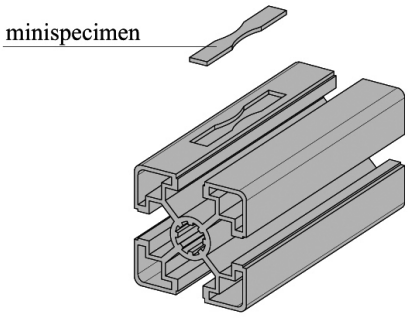

Fig. 5. A method of collecting a minispecimen from a thin-walled aluminium shaped section treated as a real structural component [14]

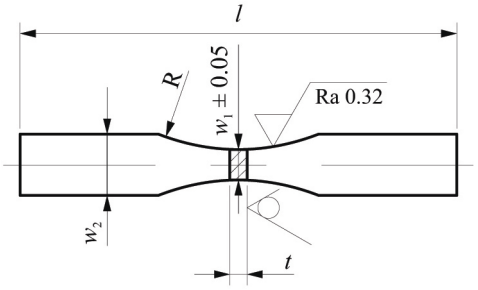

Fig. 6. Minispecimen (t = 1) and standard specimen (t = 4) used in high-cycle fatigue research

Tests were performed on specimens with a cross-sectional area consistent with the majority of standard pertaining to material fatigue [15] and a minispecimen (S_o = 3.5 mm²). Specimens featured fixed theoretical stress concentration coefficient α_k. Constant parameters of the technological process were retained. See Fig. 6 and Table 2 for geometries of flat specimens used in the fatigue tests. The analyses were performed for the standard specimen and the minispecimen made of aluminium alloy EN AW-6063. The high-cycle fatigue tests used a load variation cycle with cycle asymmetry coefficient R = 0.1, which eliminated the buckling of the minispecimen [16]. The resulting experimental data were approximated to the commonly applied forms of the linear regression equation [17].

Table 2. Specimen dimensions

	t [mm]	w_1 [mm]	w_2 [mm]	R [mm]	l [mm]	Cross-section area, S_o [mm²]
Standard specimen	4	7	14	50	100	28
Minispecimen	1	3.5	7	25	50	3.5

3.3. Results and analysis

The experimental research demonstrated the existence of an important influence of the size effect for both monotonic and fatigue loading. The verification of the accuracy of implementation of the model consisted in the estimation of fatigue strength of the standard specimen.

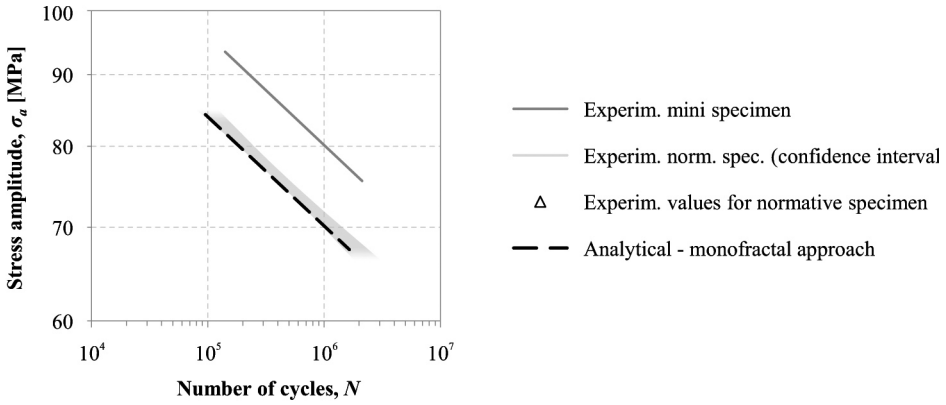

Fig. 7. Fatigue characteristics σ_a-N determined based on the experimental research and based on the analytical model of the size effect

Research computations used the experimental results for the minispecimen. The model was analysed in reference to the specimen cross-sectional area S_o. The monofractal approach under research is the determination of results of the experimental research of the size effect (at least two cross-section areas) for a given group of materials for the mean value of the fractal dimension based on literature data. The results obtained for aluminium alloy EN AW-6063 feature high consistency with the experimental data. See Fig. 7 for a summary of fatigue characteristics determined experimentally and analytically.

Conclusion

The paper presents a selection of information about the size effect in strength computations, focused on the area of computations made for high-cycle fatigue. The following four remarks wrap up the foregoing work:

a) The size effect is very often neglected in analytical computations, which is a direct result (as shown in Fig. 1c) of the low probability of obtaining material data for particularly small and particularly large objects.
b) It has been demonstrated that the literature describes a number of analytical models enabling the estimation of material data for cross-sections significantly different from sizes attributed to the standard specimens.
c) The cited example of the aluminium section and specimens produced from it, compared to the four times thicker standard specimens, is indicative of occurrence of coefficients K_S =1.15 and K_{HC} = 1.13, which means that the actual strength of a structural component is, in this case, 15% higher for static loads and 13% higher for fatigue loads than the strength to be expected based on material tests performed on the standard specimens.
d) The monofractal model, selected based on the author's own experience with aluminium, enabled the estimation of values to be expected for the "conditions" of the standard specimen based on the minispecimen tests. The result was shown graphically in Fig. 7, which visualizes a "far-going satisfactory response of the model" and the numerical data that have been obtained can be considered correct and sufficiently precise.

References

1. Carpinteri A., Spagnoli A.: Size effect in S-N curves: A fractal approach to finite-life fatigue strength. International Journal of Fatigue, 2009, 31, 927–933.
2. Tomaszewski T., Sempruch J., Piątkowski T.: Verification of selected models of size effect based on high-cycle fatigue testing on mini specimens made of EN AW-6063 aluminum alloy. Journal of Theoretical and Applied Mechanics, 2014, 52(4), 883–894.
3. Schijve J.: Fatigue of Structures and Materials. Springer, 2nd edition, 2009.
4. Shigley J.E., Mischke C.R., Brown Jr. T.H.: Standard Handbook of Machine Design. Third Edition. McGraw-Hill, New York 2004.
5. Kocańda S., Szala J.: Podstawy obliczeń zmęczeniowych, PWN, Warszawa 1997.
6. Lee Y., Pan J., Hathaway R.B., Barkey M.E: Fatigue Testing and Analysis. Theory and Practice New York, 2005.

7. Niezgodziński M.E., Niezgodziński T.: Obliczenia zmęczeniowe elementów maszyn. Państwowe Wydawnictwo Naukowe, Warszawa 1973.
8. Stephens R.I., Fatemi A., Stephens R.R., Fuchs H.O.: Metal Fatigue in Engineering. 2nd edition. Wiley Interscience, New York 2000.
9. Weibull W.: A statistical representation of fatigue failures in solids. Transaction of the Royal Institute of Technology, 27, 1949.
10. Kuguel R.: A relation between the theoretical stress concentration factor and the fatigue notch factor deduced from the concept of highly stressed volume. ASTM Proceeding. 1961, 61, 732–748.
11. Wallin K.: Statistical aspects of fatigue life and endurance limit. Fatigue & Fracture of Engineering Materials & Structures. 2010, 33(6), 333–344.
12. Makkonen L., Rabb R., Tikanmäki M.: Size effect in fatigue based on the extreme value distribution of defects. Materials Science & Engineering A. 2014, 594, 68–71.
13. Tomaszewski T.: Wykorzytsanie minipróbek do wyznaczania trwałości i wytrzymałości zmęczeniowej. Rozprawa doktorska, 2015.
14. Tomaszewski T., Sempruch J.: Wyznaczenie charakterystyki zmęczeniowej materiału profili aluminiowych z wykorzystaniem minipróbek. Przegląd Mechaniczny, 2014, 4, 28–31.
15. PN-74/H-04327. Badanie metali na zmęczenie. Próba osiowego rozciągania – ściskania przy stałym cyklu obciążeń zewnętrznych.
16. Tomaszewski T., Sempruch J.: Verification of the fatigue test method applied with the use of mini specimen. Key Engineering Materials, 2014, 598, 243–248.
17. Strzelecki P.: Verification of Accelerated Methods for Determining the S-N Curve. Applied Mechanics and Materials, 2012, 232, 8–13.